

Detection of 25 new rotating radio transients at 111 MHz

S. A. Tyul'bashev, V. S. Tyul'bashev, and V. M. Malofeev

Lebedev Physical Institute, Astro Space Center, Pushchino Radio Astronomy Observatory, 142290 Moscow Region, Russia
e-mail: serg@prao.ru

Received 26 March 2018 / Accepted 15 July 2018

ABSTRACT

Nearly all fast rotating radio transients (RRAT) that are pulsars with rare pulses have previously been detected using decimeter wavelengths. We present here 34 transients detected at meter wavelengths in our daily monitoring at declinations $-9^\circ \leq \delta \leq +42^\circ$. Twenty-five transients are new RRATs. We confirm the detection of 7 RRATs based on our early observations. One of the 34 detected transients was determined to be a new pulsar, J1326+3346. At the same time, of the 35 RRATs detected at the decimeter wavelengths in the studied area, only one was detected by us, J1848+1518. The periods of 6 RRATs were found from the arrival time of single pulses. Three quarters of all RRATs were observed more than once, and the total number of RRATs in the area we studied has doubled.

Key words. stars: neutron – pulsars: general

1. Introduction

The detection of fast radio transients in archival records of the Parkes Pulsar Survey resulted in the discovery of two classes of objects. The first group, rotating radio transients (RRAT), was determined to consist of galactic objects. These are pulsars with rare pulses (with intervals between pulses in the range of minutes or hours; [McLaughlin et al. 2006](#)). The second group was fast radio bursts (FRB), which are rarer objects of an extragalactic nature ([Lorimer et al. 2007](#)).

The duration of flares of the RRATs and FRB objects is comparable; the timescale is from a fraction of a millisecond to tens of milliseconds, while the observed dispersion measures (DM) appreciably differ (see catalogues ATNF¹, [Manchester et al. 2005](#); RRATalog²; FRBcat³, [Petroff et al. 2016](#)). Whereas the dispersion measures' intervals for known pulsars, $2.38 < DM < 1778 \text{ pc cm}^{-3}$ (ATNF), and for RRATs, $9.2 < DM < 786 \text{ pc cm}^{-3}$ (RRATalog), are rather similar, this interval is offset for FRBs toward higher values, $176.4 < DM < 1629.18 \text{ pc cm}^{-3}$ (FRBcat). To distinguish RRATs, the first turn is examined for repeated pulses and the pulsar period is determined. If the period cannot be determined, the separation of the RRAT and FRB can be achieved using the model of the thermal electron distribution in the Galaxy ([Cordes & Lazio 2002](#); [Yao et al. 2017](#)), and in the case of the new source, the observed dispersion measure is compared with the measure expected in that direction. If the observed value is considerably higher than expected, an FRB is detected. From the point of view of the observer, the search for fast radio transients, either RRATs or FRB, is essentially a search for single pulses from pulsars. If we recall history, the discovery itself of pulsars as a new class of objects took place after the detection of their single pulses ([Hewish et al. 1968](#)).

So far, fast transients (RRATs/FRBs) have been found mostly in the decimeter wavelength range using the largest telescopes in the world, the 64 m Parkes, the 100 m Green Bank,

and the 300 m Arecibo telescope (see, e.g. [Keane et al. 2010](#); [Karako-Argaman et al. 2015](#); [Deneva et al. 2016](#)). Dedicated searches for RRATs/FRBs were also carried out in the meter wavelength range at the Low Frequency ARray (LOFAR), but the result was negative ([Karastergiou et al. 2015](#)). Meanwhile, the sensitivity of LOFAR and higher frequency surveys are comparable. The first RRAT detection at meter wavelengths was made in Pushchino at the Large Phased Array radio telescope ([Shitov et al. 2009](#)) before the new daily monitoring survey was started.

The optimal combination of conditions for the search of fast transients includes a high instantaneous sensitivity of the radio telescope, because fast transients are, as a whole, rather faint objects; a short sampling interval comparable with the pulse duration; and a multichannel receiver with a narrow band of each frequency channel to reduce pulse broadening due to the dispersion measure. These conditions are partly satisfied in the monitoring survey initiated in 2013 at the Large Phased Array of the Lebedev Physical Institute (LPA LPI) at a frequency of 111 MHz. The aim was to forecast the time of arrival of coronal mass ejections from the Sun on the basis of observations of scintillating radio sources ([Shishov et al. 2016](#); Space Weather Project). The survey covered an area of about 17 000 square degrees daily. The data from the survey were also used for the search of pulsars and transients. Two independent groups have discovered 41 pulsars ([Tyul'bashev et al. 2016, 2017](#); [Rodin et al. 2017](#)).

In 2017, a test search for RRATs in daily monitoring data was also performed using 5 days (1–5 September 2015; [Tyul'bashev & Tyul'bashev 2017](#)) and 28 days (1–28 September 2015; [Tyul'bashev et al. 2018](#)). As a result, 54 fast transients have been detected; of these, 7 RRATs were absent in ATNF and RRATalog, and 47 have been identified with known pulsars. In this paper, we present the results of our search for new fast transients after processing six months of monitoring data.

2. Observations and results

Our monitoring observations were conducted using 96 beams simultaneously covering about 40 square degrees in the sky at

¹ <http://www.atnf.csiro.au/people/pulsar/psrcat/>

² <http://astro.phys.wvu.edu/rratalog/>

³ <http://www.astronomy.swin.edu.au/pulsar/frbcat/>

the LPA LPI meridian telescope at a frequency of 111 MHz that commenced in August 2014. The beams covered the declination interval $-9^\circ < \delta < +42^\circ$ and the beam size was $\sim 0.5^\circ \times 1^\circ$. The data were recorded in one-hour segments. Each segment was initialized by GPS time markers, but within the hour, time was controlled by a quartz oscillator. Transients were searched for in the data recorded in a 2.5 MHz band in a 32-channel frequency mode with a sampling interval of 12.5 ms. In this mode, the fluctuation sensitivity of the telescope with an effective area of the antenna of 45 000 m² toward zenith is 0.3 Jy. The data from July–December 2015 were processed. The detailed technique of the search for the transients was described by Tyul’bashev et al. (2018). The main approach was that the data in 32 frequency channels were summed for each DM, every peak in the mean profile was registered, and a few criteria were taken into account.

The software performed searches for dispersion measures from 3 to 100 pc cm⁻³ and searched for dispersed signals with a signal-to-noise ratio (S/N) > 5.5 . A limit of the DM was taken because of the large number of false sources that exists for DM less than 3 pc cm⁻³, and we did not have any detections in our pulsar search for DM > 100 pc cm⁻³ (Tyul’bashev et al. 2016, 2017).

After the primary search, the catalog included about 300 000 objects, which were analyzed by means of the BSA-Analytics software (Qt/C++ code distributed under the GPL V3.0 license)⁴. The BSA-Analytics program during the search for transients gave the choice of a certain beam (sky direction), restrictions of the signals detected at a given S/N , and the sidereal time of the tested block. The filters of the program checked whether the transient was detected in no more than three beams, or detected only once and at only one dispersion measure, or if the main part of pixels with a high S/N was arranged along a certain dispersion measure (geometric filter), or removal of poor-quality days, or elimination from the shown catalog of the objects that were found earlier. The software also enables us to search for the RRAT period, if during the observational sessions two or more pulses per session were detected, to sum the dynamic spectra and mean profiles, to determine the pulse half-width, to save graphs, and to refine the dispersion measure by overlaying a dispersion curve with the known dispersion measure on the dynamic spectrum. This software also lends some other possibilities of usage. The ultimate control of the identified candidates was made visually for transients with a visible line of the dynamic spectra. This visible line corresponds to the value $S/N > 7$ of the pulse profile.

Additional details of the capabilities of the updated LPA LPI and of the search technique are given in Shishov et al. (2016), Tyul’bashev et al. (2017, 2018) and in the BSA-Analytics Project⁵.

Figure 1 demonstrates the sample pulses from the pulsar and the new RRAT. We consider the objects J0941+1621 and J0943+1631 separately. J0943+1631 is a known pulsar with a dispersion measure of 20.3 pc cm⁻³, and the overwhelming part of the dispersed signals with a dispersion measure of 19–20 pc cm⁻³ is visible in this direction. For some of these records, another transient appears, which can be at an arbitrary place in the dynamic spectrum graph with respect to the pulsar, and it has a different dispersion measure. For better visibility, we averaged 19 dynamic spectra and mean pulsar profiles. The red line in the averaged dynamic spectrum of the right part of the image corresponds to the dispersion measure of 19 pc cm⁻³. In the figure

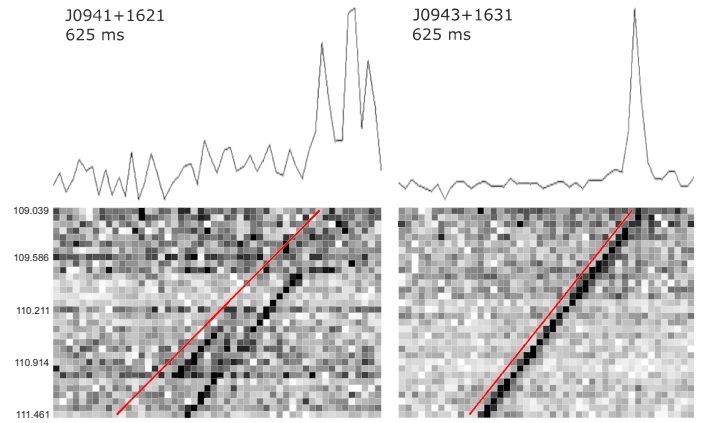


Fig. 1. Two different slopes in the dynamic spectrum in the image that corresponds to RRAT J0941+1621 and PSR J0943+1631.

with the J0941+1621 RRAT, a red line is also drawn, but it corresponds to a dispersion measure of 24 pc cm⁻³. The graphs for the RRAT J0941+1621 and pulsar J0943+1631 are placed side by side to explicitly show the different slopes of the dispersion curve of these two objects located in the same direction and having similar dispersion measures. The average profile of the figure is the sum of two different dispersion curves, and it therefore has a complex shape with a triple peak. One pixel visible in a dynamic spectrum picture has a timescale (12.5 ms) in the horizontal direction and a frequency channel bandwidth (78 kHz) in the vertical direction. The upper and lower lines of the spectra correspond to the frequencies 111.461 and 109.039 MHz, respectively, therefore the dark line in the dynamic spectrum tracing the transient extends from the top of the right corner to the bottom of the left corner. The dynamic spectrum is presented with a small margin in time. This time in milliseconds is shown below the transient name.

Table 1 lists the main parameters of the new 25 RRATs together with additional information for 8 RRATs published earlier by Samodurov et al. (2017), Tyul’bashev et al. (2018), and RRATalog. The first column contains the RRAT name in the J2000 notation. The second and third columns give the right ascension and declination of the source. The fourth column lists the estimated dispersion measure of the RRAT. In the fifth column, estimates of the observed peak flux density S_{peak} for the strongest pulses are given with corrections for the declination (zenith correction) and for the particulars of the multibeam LPA LPI directivity pattern. In the sixth column, the observed pulse half-width is given without taking into account dispersion broadening within the channel frequency band. The seventh column lists estimation of RRAT periods. These estimates were made for RRATs with a few detections of the individual pulses during one session. We measured the time distance between pulses and therefore can calculate the upper limit of the period. In the eighth column, the number of repeated events is given. In the ninth column, the references to the early detections of 8 RRATs are given. For a single detection of an RRAT, the accuracy of the coordinates in the right ascension is $\pm 2^m$. For multiple detections, the column lists the average coordinate and the rms error. The declination accuracy is indicated in the table, and the accuracy of the estimated period is ± 0.003 s. The flux density was estimated from the noise trace, therefore the accuracy of this quantity is low. It may differ from the given value by a factor of 1.5–2. For the RRATs with an estimated value for the period, we checked the presence of the signal in the cumulative Fourier power

⁴ See <https://github.com/vtyulb/BSA-analytics>

⁵ <https://bsa-analytics.prao.ru/>

Table 1. Main parameters of 33 detected RRATs.

Transient name	α_{2000}	δ_{2000}	DM (pc cm ⁻³)	S_{peak} (Jy)	W_e (ms)	P (s)	N (times)	Ref.
J0139+3310	01 ^h 39 ^m 30 ^s ± 20 ^s	33°10' ± 15'	20 ± 1	40	25	1.2473	>10	(1)
J0305+4001	03 05 26 ± 32	40 01 ± 15	24 ± 2	2.7	<12.5	–	2	
J0318+1341	03 18 35 ± 28	13 41 ± 20	12 ± 1	7.6	30	1.9740	>10	(2)
J0452+1651	04 52 56 ± 90	16 51 ± 25	19 ± 3	3.1	<12.5	–	2	
J0534+3407	05 34 30 ± 20	34 07 ± 15	24.5 ± 1.5	2.6	15	–	7	
J0609+1635	06 09 18 ± 21	16 35 ± 30	85 ± 3	2.3	55	–	>10	
J0625+1730	06 25 19 ± 90	17 30 ± 25	58 ± 4	4.3	25	–	3	
J0640+0744	06 40 40 ± 35	07 44 ± 25	52 ± 3	8.7	35	–	>10	(2)
J0803+3410	08 03 05 ± 85	34 10 ± 15	34 ± 2	3.4	25	–	5	
J0941+1621	09 41 30	16 21 ± 20	23 – 24	–	??	–	>10	
J1005+3015	10 05 30 ± 40	30 15 ± 15	17.5 ± 1.5	28.3	30	–	>10	(1)
J1132+0921	11 32 00	09 21 ± 20	22 ± 2	7.3	40	–	1	
J1132+2515	11 32 50 ± 30	25 15 ± 15	23 ± 3	6.2	20	1.0020	>10	
J1329+1349	13 29 00	13 49 ± 20	12 ± 2	11.3	15	–	1	(2)
J1336+3346	13 36 26 ± 50	33 46 ± 15	8 ± 1	8.4	15	3.0130	>10	(2)
J1346+0622	13 46 00	06 22 ± 25	8 ± 1	11.6	<12.5	–	1	
J1400+2127	14 00 18 ± 30	21 27 ± 15	10.5 ± 1	24.5	25	–	9	
J1404+1210	14 04 49 ± 38	12 10 ± 20	17 ± 1	10.4	–	2.6505	>10	
J1502+2813	15 02 09 ± 40	28 13 ± 15	14 ± 1.5	16.3	25	3.7840	>10	
J1555+0108	15 55 58 ± 17	01 08 ± 25	18.5 ± 1.5	22.6	20	–	3	(2)
J1732+2700	17 32 24 ± 41	27 00 ± 15	36.5 ± 1.5	5.9	25	–	7	
J1841-0448	18 41 10 ± 20	–04 48 ± 25	29 ± 3	3.8	15	–	>10	
J1848+1518	18 48 42 ± 90	15 18 ± 20	75 ± 5	2.3	25	–	2	(3)
J1917+1723	19 17 30	17 23 ± 20	38 ± 3	2.8	25	–	1	
J1930+0104	19 30 30	01 04 ± 25	42 ± 3	4.9	30	–	1	
J2052+1308	20 52 21 ± 40	13 08 ± 20	42 ± 3	2.9	20	–	3	
J2105+1917	21 05 20 ± 20	19 21 ± 20	33 ± 3	2.7	25	–	10	
J2107+2606	21 07 30	26 06 ± 20	10.5 ± 2	3.1	25	–	1	
J2135+3032	21 35 00	30 32 ± 15	63 ± 2	3.5	50	–	1	
J2146+2148	21 46 00	21 48 ± 20	43 ± 3	2.5	20	–	1	
J2202+2147	22 02 21 ± 21	21 47 ± 20	17 ± 2	4.8	<12.5	–	8	
J2205+2244	22 05 30	22 44 ± 20	22 ± 2	3.0	40	–	1	
J2210+2118	22 10 07 ± 90	21 18 ± 20	45 ± 3	2.6	<12.5	–	3	

References. (1) Samodurov et al. (2017), (2) Tyul'bashev et al. (2018), (3) RRATalog.

spectra obtained for six-channel frequency data with a sampling interval of 0.1 s (Tyul'bashev et al. 2017). We have found no harmonics for the periods listed in the table. We have also tried averaging with the known period and dispersion measure for the days when multiple transients pulses were observed, taking into consideration that we might have detected flaring pulsars. In the process of averaging over an observational session, we did not manage to obtain mean profiles. Figure 2 presents 25 of the 33 RRATs from Table 1, except for the 7 RRATs detected earlier in our daily monitoring and RRAT J0941+1621 (Fig. 1).

We also found 11 strong pulses for transient J1326+3346. This is probably a new pulsar. The preliminary estimation period and dispersion measure for the candidate were $DM = 4 \pm 1 \text{ pc cm}^{-3}$ and period $P = 41 \text{ ms}$, respectively. The coordinates of the pulsar are $\alpha_{2000} = 13^{\text{h}}26^{\text{m}}42^{\text{s}}$, $\delta_{2000} = 33^{\circ}46'$ and the coordinate accuracy is the same as that of the RRATs. A full search of the signal with $0 < DM < 8 \text{ pc cm}^{-3}$ and a period near 41 ms was performed. We confirm the detection of a new pulsar and refine the period ($P = 41.5 \text{ ms}$). The dynamic spectrum of PSR J1326+3346 and mean profile are shown in Fig. 3. The time resolution in our monitoring program is low, therefore no details in the observed profile in the left panel can be identified.

Minimum and maximum of observed dispersion measure at transients J1326+3346 ($DM = 4 \text{ pc cm}^{-3}$) and J0609+1635 ($DM = 85 \text{ pc cm}^{-3}$). The distances to the new RRATs were estimated using the NE2001 model for the electron density distribution in the Galaxy (Cordes & Lazio 2002)⁶. These distances do not show any peculiarities. The median distance to the transients was determined to be $R = 1.238 \text{ kpc}$ (for RRAT J2202+2147). The nearest source is PSR J1326+3346 ($R = 0.47 \text{ kpc}$), and the most distant is RRAT J2135+3032 ($R = 3.888 \text{ kpc}$).

In addition to the detected new RRATs (see Table 1 and Fig. 2) that are not included in the known catalogs of pulsars and transients (ATNF, RRATalog, and FRBcat), we found individual pulses from 103 pulsars. The analysis of these pulsars will be presented in subsequent papers. The images of the dynamic spectra and short information about each pulsar are presented online⁷. For comparison, the ATNF catalog contains 420 pulsars with declinations $-9^{\circ} < \delta < 42^{\circ}$ and $DM < 100 \text{ pc cm}^{-3}$. Then we observed 25% of these pulsars as transients, which indicates the high efficiency of the pulsar search using individual pulses

⁶ <https://www.nrl.navy.mil/rsd/RORF/ne2001/index.html>

⁷ <https://bsa-analytics.prao.ru/transients/pulsars.php?lang=eng>

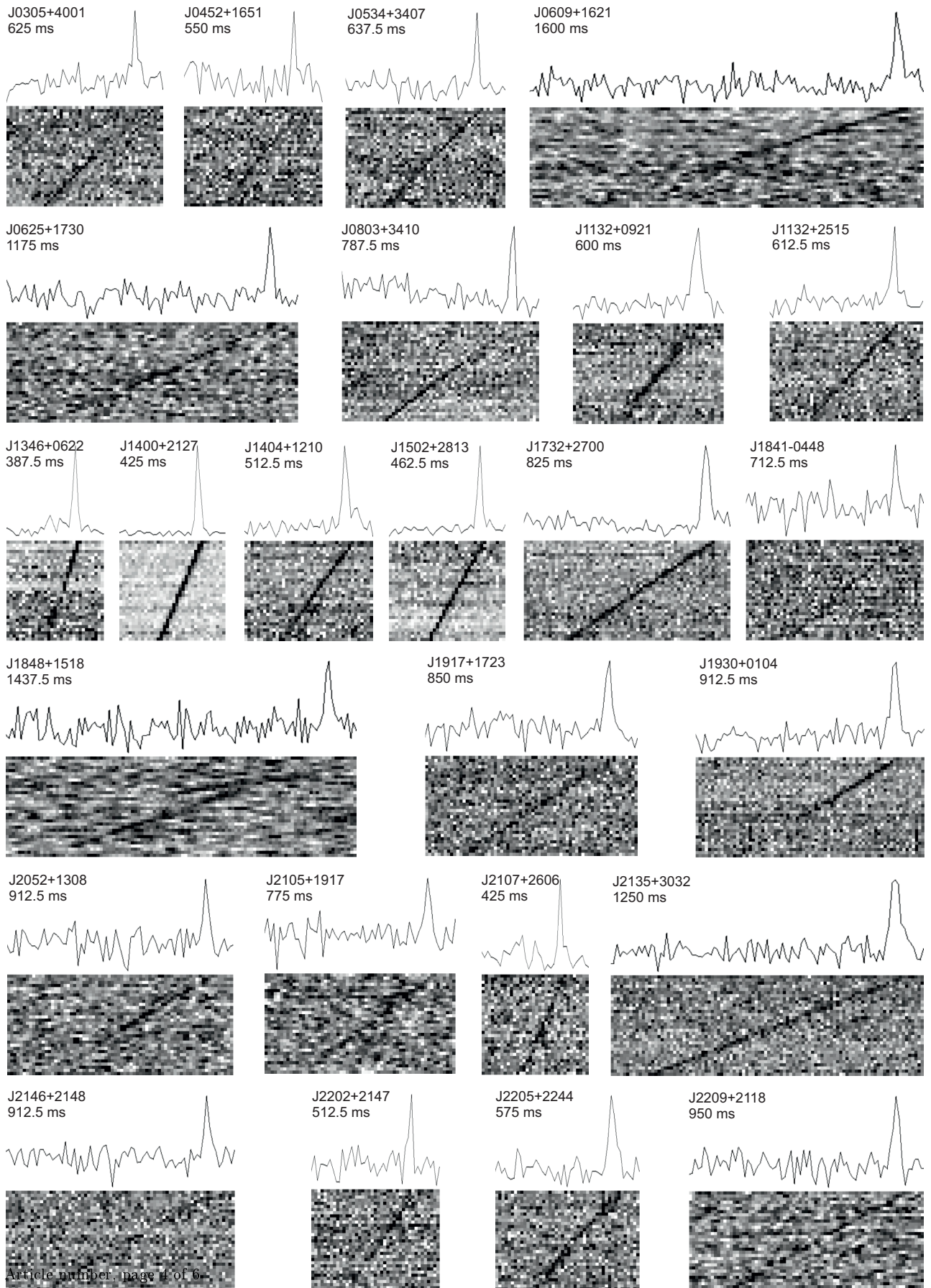


Fig. 2. 25 RRATs from Table 1. The average profile, dynamic spectrum, and recording duration are represented for each RRAT.

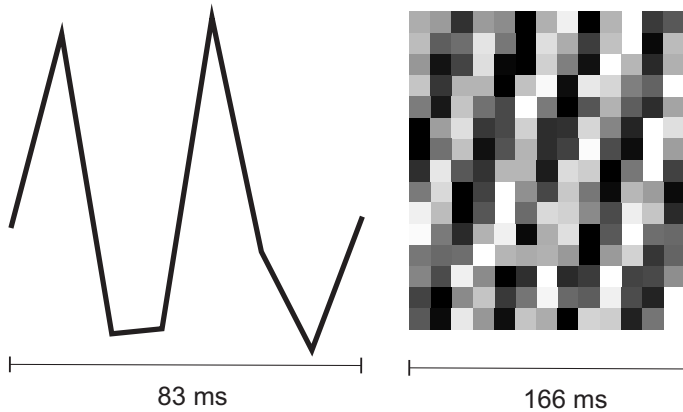


Fig. 3. Dynamic spectrum of PSR J1326+3346 (*right panel*) obtained by adding a period of $4 \times 41.5 = 166$ ms for the best day using the program for the pulsar search (Tyul'bashev et al. 2016, 2017). The mean profile with the double period is presented in the *left panel*.

at a meter wavelength. The efficiency of this method of pulsar search is comparable with our method of accumulated Fourier spectra, because we have found 131 known pulsars in three years (Tyul'bashev et al. 2017).

It should be noted that in the processed data, many faint RRAT candidates remain. These objects have appeared several times; in their dynamic spectrum, the dispersion curve is virtually invisible. Therefore, they were not included in this work. We may expect that with an increase in the number of processed days, additional repeated events will be observed in the same directions and at the same dispersion measures, and the total number of RRATs can thus grow by a factor of a few.

3. Discussion and conclusion

The appearance of the dynamic spectrum and the obtained mean profile of one of the detected fast transients (J1326+3346) suggest the existence of a new fast pulsar ($P = 41.5$ ms). This pulsar could not be identified in the summary power spectra (Tyul'bashev et al. 2017) because using this technique, the minimum possible period was 200 ms. The dispersion measures of all discovered transients do not contradict the NE2001 model. In this case, we conclude that all our radio transients (Table 1) belong to the RRATs group, but not to FRBs.

We have compared the list of the objects from RRATalog with the objects detected by our group and found coincidence for three sources. In particular, in this catalog, the object J0301+2052 with $DM = 19 \text{ pc cm}^{-3}$ and $P = 1.207$ s is classified as an RRAT. In our pulsar search (Tyul'bashev et al. 2016) we found the pulsar J0303+2248 with the same dispersion measure and period. This is apparently the same object. A possible transition from RRAT to pulsars in observations at a lower frequency was indicated in Deneva et al. (2009). In RRATalog the source J1538+2345 is classified as an RRAT; in our observations, however, it has been detected on more than one hundred occasions, both as a pulsar and an RRAT. In the ATNF catalog, the source J1538+2345 is also listed as a pulsar. These two sources are not included in our list (Table 1 and Figs. 1–3). The RRAT J1848+1518 ($DM = 75 \text{ pc cm}^{-3}$) apparently coincides with RRATalog source J1849+1517 ($DM = 77.4 \text{ pc cm}^{-3}$), and it is the only RRAT from the full list of RRATs (RRATalog) that

is included in our list and in Fig. 2. We did not detect RRAT J2225+35 found by LPA in observations made in 2004 and 2006 by the group of Yu. P. Shitov (Shitov et al. 2009). Most likely, this indicates its low duty factor: one pulse in more than 10 h (the total time of LPA observations at each sky point for a six-month period). Considering the comparable sensitivity of the Parkes and LPA antennas (Table 1 in Tyul'bashev et al. 2018), we may expect similar duty factors. It should be kept in mind that among pulsars, objects have recently been detected with very infrequent, strong bursts of pulses. Thus, for PSR J0653+8051, two flares have been observed with a total duration of about 5 min in 400 days of observations; this is about 0.3% of the total observational time and is equivalent to one strong pulse in 6.5 h of continuous record (Malofeev et al. 2016).

Keane & Kramer (2008) estimated the possible quantity of observed RRATs (non-canonical part of the full pulsar sample; Karako-Argaman et al. 2015), which is twice as high as the quantity of ordinary (canonical) pulsars. If the flux density distribution of the individual RRAT pulses is the same as that of pulsars, and taking into account our detection of individual pulses from 103 known pulsars, we can estimate that only 15% of RRATs with an $S/N > 7$ that were available for observations at LPA were detected.

The main result of our rotating radio transients search at the 111 MHz frequency is the detection of 25 RRATs, the confirmation of 8 RRATs determined from previous detections, and the detection of one ms pulsar J1326+3346. The period estimates were made for 3 out of 25 new RRATs, and for 3 out of 8 RRATs detected previously. We found that 16 new RRATs show more than one event, but the remaining 9 RRATs were registered only once.

Acknowledgements. The authors thank L.B. Potapova and G.E. Tyul'basheva for help with the manuscript and figures. This work was supported by the Russian Foundation for Basic Research (project codes 16-02-00954), and by the Program of the Presidium of the Russian Academy of Sciences "Transition and Explosive Processes in Astrophysics".

References

- Cordes, J., & Lazio, T. 2002, ArXiv e-prints [arXiv:astro-ph/0301598]
Deneva, J., Cordes, J., McLaughlin, M., et al. 2009, *ApJ*, 703, 2259
Deneva, J., Stovall, K., McLaughlin, M., et al. 2016, *ApJ*, 821, 10
Hewish, A., Bell, S., Pilkington, J., Scott, P., & Collins, R. 1968, *Nature*, 217, 709
Karako-Argaman, C., Kaspi, V., Lynch, R., et al. 2015, *ApJ*, 809, 67
Karastergiou, A., Chennamangalam, J., Armour, W., et al. 2015, *MNRAS*, 452, 1254
Keane, E. F., & Kramer, M. 2008, *MNRAS*, 391, 2009
Keane, E., Ludovici, D., Eatough, R., et al. 2010, *MNRAS*, 401, 1057
Lorimer, D., Bailes, M., McLaughlin, M., Narkevic, D., & Crawford, F. 2007, *Science*, 318, 777
Malofeev, V., Teplykh, D., Malov, O., & Logvinenko, S. 2016, *MNRAS*, 457, 538
Manchester, R., Hobbs, G., Teoh, A., & Hobbs, M. 2005, *AJ*, 129, 1993
McLaughlin, M., Lyne, A., Lorimer, D., et al. 2006, *Nature*, 439, 817
Petroff, E., Barr, E., Jameson, A., et al. 2016, *PASA*, 33, 45
Rodin, A., Oreshko, V., & Samodurov, V. 2017, *Astron. Rep.*, 61, 30
Samodurov, V., Pozanenko, A., Rodin, A., et al. 2017, *Commun. Comp. Inform. Sci. Ser.*, 706, 130
Shishov, V., Chashei, I., Oreshko, V., et al. 2016, *Astron. Rep.*, 60, 1067
Shitov, Y., Kuzmin, A., Dumskii, D., & Losovsky, B. 2009, *Astron. Rep.*, 53, 561
Tyul'bashev, S., & Tyul'bashev, V. 2017, *Astronomicheskii Tsirkulyar*, 1636, 1
Tyul'bashev, S., Tyul'bashev, V., Oreshko, V., & Logvinenko, S. 2016, *Astron. Rep.*, 60, 220
Tyul'bashev, S., Tyul'bashev, V., Kitaeva, M., et al. 2017, *Astron. Rep.*, 61, 848
Tyul'bashev, S., Tyul'bashev, V., Malofeev, V., et al. 2018, *Astron. Rep.*, 62, 63
Yao, J., Manchester, R., & Wang, N. 2017, *ApJ*, 835, 29